Chinese Physics Letters **40**, 127401 (2023) **Express Letter**

Effective Bi-Layer Model Hamiltonian and Density-Matrix Renormalization Group Study for the High-T_c Superconductivity in $La_3Ni_2O_7$ under High Pressure

Yang Shen(沈阳)[1], Mingpu Qin(秦明普)[1,2*], and Guang-Ming Zhang(张广铭)[3,4*]

[1]*Key Laboratory of Artificial Structures and Quantum Control, School of Physics and Astronomy, Shanghai Jiao Tong University, Shanghai 200240, China*
[2]*Hefei National Laboratory, Hefei 230088, China*
[3]*State Key Laboratory of Low-Dimensional Quantum Physics and Department of Physics, Tsinghua University, Beijing 100084, China*
[4]*Frontier Science Center for Quantum Information, Beijing 100084, China*

(Received 2 November 2023; accepted manuscript online 14 November 2023)

High-T_c superconductivity with possible $T_c \approx 80$ K has been reported in the single crystal of $La_3Ni_2O_7$ under high pressure. Based on the electronic structure given by the density functional theory calculations, we propose an effective bi-layer model Hamiltonian including both $3d_{z^2}$ and $3d_{x^2-y^2}$ orbital electrons of the nickel cations. The main feature of the model is that the $3d_{z^2}$ electrons form inter-layer σ-bonding and anti-bonding bands via the apical oxygen anions between the two layers, while the $3d_{x^2-y^2}$ electrons hybridize with the $3d_{z^2}$ electrons within each NiO_2 plane. The chemical potential difference of these two orbital electrons ensures that the $3d_{z^2}$ orbitals are close to half-filling and the $3d_{x^2-y^2}$ orbitals are near quarter-filling. The strong on-site Hubbard repulsion of the $3d_{z^2}$ orbital electrons gives rise to an effective inter-layer antiferromagnetic spin super-exchange J. Applying pressure can self dope holes on the $3d_{z^2}$ orbitals with the same amount of electrons doped on the $3d_{x^2-y^2}$ orbitals. By performing numerical density-matrix renormalization group calculations on a minimum setup and focusing on the limit of large J and small doping of $3d_{z^2}$ orbitals, we find the superconducting instability on both the $3d_{z^2}$ and $3d_{x^2-y^2}$ orbitals by calculating the equal-time spin singlet pair–pair correlation function. Our numerical results may provide useful insights in the high-T_c superconductivity in single crystal $La_3Ni_2O_7$ under high pressure.

DOI: 10.1088/0256-307X/40/12/127401

The successfully synthesized infinite-layer nickelate superconductors[1–7] have provided another platform for research of the microscopic origin of unconventional superconductivity. Similar to high-T_c cuprates, the infinite-layer nickelates with nominal Ni^+ ($3d^9$) cations contain $3d_{x^2-y^2}$ orbital degrees of freedom on a quasi-two-dimensional Ni–O square lattice.[8,9] However, the electronic states of oxygen $2p$ orbitals are far below the Fermi level and have a much reduced $3d$–$2p$ mixing due to the larger separation of their on-site energies, and their low-energy electronic structures are more likely to fall into the Mott–Hubbard than the charge-transfer regime with a super-exchange energy being at least an order of magnitude smaller than in cuprates.[10] As a consequence, the parent infinite-layer nickelates may be modeled as a self-doped Mott insulator with two types of charge carriers, and the low-temperature upturn of the electric resistivity[1,11] arises from the magnetic spin scattering between low-density conduction electrons from the rare earths and localized Ni-$3d_{x^2-y^2}$ magnetic moments.[12,13] Upon Sr doping, the superconducting T_c is just around 9–15 K in the $Nd_{0.8}Sr_{0.2}NiO_2$ thin films,[1] and the maximum T_c of 31 K has been achieved in $Pr_{0.82}Sr_{0.18}NiO_2$ films under high pressure.[14] So far, no bulk crystals can be synthesized and show superconductivity.

Recently, it has been reported that the superconductivity with possible $T_c \approx 80$ K is observed in the single crystal of $La_3Ni_2O_7$ with pressure between 14.0 and 43.5 GPa using high-pressure resistance and mutual inductive magnetic susceptibility measurements.[15] Density functional theory (DFT) calculations for the two nearest intra-layer Ni cations in a bilayer Ruddlesden–Popper (RP) phase[15,16] have suggested that both the $3d_{x^2-y^2}$ and $3d_{z^2}$ orbitals of Ni cations strongly mix with oxygen $2p$ orbitals. The $3d_{z^2}$ orbitals via the apical oxygen usually have a large inter-layer coupling due to the quantum confinement of the NiO_2 bilayer in the structure, and the resulting energy splitting of Ni cations can dramatically change the distribution of the averaged valence state of $Ni^{2.5+}$. The numerical results further indicated that the superconductivity emerges coincidently with the metallization of the σ-bonding bands under the Fermi level, consisting of the $3d_{z^2}$ orbitals with the apical oxygen connecting Ni–O bilayers.[17,18] These distinct features are important clues for the high-T_c superconductivity in this RP double-layered perovskite nickelates, which are different from the infinite-layer nickelate superconductors.

In this work, based on the DFT electronic

*Corresponding authors. Email: qinmingpu@sjtu.edu.cn; gmzhang@tsinghua.edu.cn
© 2023 Chinese Physical Society and IOP Publishing Ltd

structure,[15,16] we propose an effective bi-layer model Hamiltonian including both $3d_{z^2}$ and $3d_{x^2-y^2}$ orbital electrons of the nickel cations, which are different from the single orbital bi-layer Hubbard model.[19–27] The main feature of the model is that the $3d_{z^2}$ electrons form inter-layer σ-bonding and anti-bonding bands via the apical oxygen anions between two layers, while the $3d_{x^2-y^2}$ electrons hybridize with the $3d_{z^2}$ electrons within each NiO_2 plane. Due to their special spatial symmetries of two e_g orbitals, the intra-layer hopping of the $3d_{z^2}$ orbital electrons and the inter-layer hopping of the $3d_{x^2-y^2}$ orbital electrons are very small, and can be neglected. The chemical potential difference of these two orbital electrons ensures that the $3d_{z^2}$ orbitals are close to half-filling and the $3d_{x^2-y^2}$ orbitals are near quarter-filling. The strong on-site Hubbard repulsion gives rise to an inter-layer antiferromagnetic super-exchange of the $3d_{z^2}$ orbital electrons J. Applying pressure can increase the coupling strength J and self-dope additional holes on the $3d_{z^2}$ orbitals with the same amount of electrons doped on the $3d_{x^2-y^2}$ orbitals. By performing numerical density-matrix renormalization group (DMRG) calculations on a minimum one-dimensional setup and focusing on the large J and small doping of $3d_{z^2}$ orbital limit, we observe a charge-density wave (CDW) for both $3d_{z^2}$ and $3d_{x^2-y^2}$ electrons but with different wavelengths. We also find instability of superconductivity for both orbitals from the equal-time spin singlet pair–pair correlations. We attribute the pairing on $3d_{z^2}$ orbital to the formation of inter-layer singlet pairs, and the pairing on $3d_{x^2-y^2}$ orbitals from the hybridization of the two orbitals.

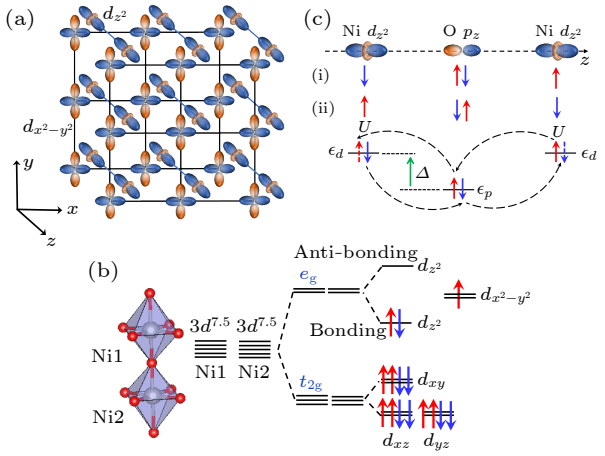

Fig. 1. (a) Schematic illustration of the $3d_{x^2-y^2}$ and $3d_{z^2}$ orbitals of Ni cations. We have omitted the p_x and p_y orbitals of oxygen anions in the xy plane and the p_z orbitals of the apical oxygen anions between the two layers. (b) The energy levels for two $3d$ orbitals of Ni cations in one unit cell. (c) The antiferromagnetic spin super-exchange coupling resulted from the effective interactions between the two inter-layer $3d_{z^2}$ orbitals of Ni cations via the apical oxygen p_z orbitals. We just list the two low-energy states and the higher energy intermediate processes, leading to the effective interaction Eq. (2).

Effective Model Hamiltonian. Let us focus on the bi-layer RP bulk single crystals of $La_3Ni_2O_7$ [see Figs. 1(a) and 1(b)]. A simple electron count gives $Ni^{2.5+}$, i.e., $3d^{7.5}$ state for both Ni cations, and the previous experiments indicated that $La_3Ni_2O_7$ is a paramagnetic metal. $Ni^{2.5+}$ is usually believed to be given by mixed valence states of Ni^{2+} ($3d^8$) and Ni^{3+} ($3d^7$), corresponding to the half-filled of both $3d_{z^2}$ and $3d_{x^2-y^2}$ orbitals and singly occupied $3d_{z^2}$ with empty $3d_{x^2-y^2}$ orbitals, respectively. With a bilayer RP phase, two $3d_{z^2}$ orbitals via apical oxygen anions usually have a large inter-layer coupling due to the quantum confinement of the NiO_2 bilayer in the structure, which causes a large energy splitting of Ni cations, see Fig. 1(c). Then the distribution of the averaged valence state of $Ni^{2.5+}$ can be dramatically changed.

We first consider an isolated Ni–O–Ni three-site system, which includes only the half-filled $3d_{z^2}$ orbitals [see Fig. 1(c)],

$$H = v\sum_{\sigma}(d^{\dagger}_{2\sigma}p_{\sigma} - d^{\dagger}_{1\sigma}p_{\sigma} + \text{h.c.}) + \epsilon_p n_p + \epsilon_d(n_{d1} + n_{d2}) + Un_{d1\uparrow}n_{d1\downarrow} + Un_{d2\uparrow}n_{d2\downarrow}, \quad (1)$$

where v is the hybridization between the $3d_{z^2}$ orbital of nickel and the p_z orbital of apical oxygen, ϵ_d (ϵ_p) is the energy for the $3d_{z^2}$ (p_z) orbital, and U is the on-site Coulomb repulsion for the $3d_{z^2}$ orbital of nickel. Notice that the signs for hybridization are different for the two $3d_{z^2}$ orbitals. When $U \gg v, \epsilon_p, \epsilon_d$, the lower energy configurations are shown in (i) and (ii) in Fig. 1(c), where the oxygen p_z orbital is doubly occupied and the $3d_{z^2}$ orbital is half-filled. The state of these two $3d_{z^2}$ orbitals occupied by parallel electrons has a higher energy. By considering the virtual transition to higher energy states, we can derive an anti-ferromagnetic super-exchanges between these two $3d_{z^2}$ orbitals as

$$H_{\text{eff}} = J\boldsymbol{S}_1 \cdot \boldsymbol{S}_2, \quad (2)$$

with

$$J = \frac{4v^4}{(U+\Delta)^2}\left(\frac{1}{U} + \frac{1}{U+\Delta}\right), \quad \Delta = \epsilon_d - \epsilon_p. \quad (3)$$

Then a simplified bi-layer model Hamiltonian of a square planar coordinated Ni cations consisting of the $3d_{z^2}$ and $3d_{x^2-y^2}$ orbitals characterizes the effective low-energy physics,

$$\begin{aligned} H = &- t_{x^2-y^2}\sum_{\langle ij\rangle,\sigma,a=1,2}(c^{\dagger}_{a,i,\sigma}c_{a,j,\sigma} + \text{h.c.}) \\ &- \mu_{x^2-y^2}\sum_{i,a=1,2} n^c_{a,i} + U\sum_{i,a=1,2} n^c_{a,i\uparrow}n^c_{a,i\downarrow} \\ &- t_{x^2-y^2,z^2}\sum_{i,\sigma,a=1,2}(d^{\dagger}_{a,i,\sigma}\widetilde{c}_{a,i,\sigma} + \text{h.c.}) \\ &- t_{z^2}\sum_{i,\sigma}(d^{\dagger}_{1,i,\sigma}d_{2,i,\sigma} + \text{h.c.}) \\ &+ J\sum_i \boldsymbol{S}^d_{1,i}\cdot\boldsymbol{S}^d_{2,i} - \mu_{z^2}\sum_{i,a} n^d_{a,i}, \end{aligned} \quad (4)$$

with $c^{\dagger}_{a,i,\sigma}$ ($d^{\dagger}_{a,i,\sigma}$) creates a $3d_{x^2-y^2}$ ($3d_{z^2}$) electron at the i-th site for the layer $a = 1, 2$, $\widetilde{c}_{a,i,\sigma} = (c_{a,i+x,\sigma} + c_{a,i-x,\sigma} - c_{a,i+y,\sigma} - c_{a,i-y,\sigma})/2$, t_{z^2} is the hopping for the $3d_{z^2}$ electron between the two layers and is set as the energy unit, $t_{x^2-y^2}$ is the hopping for the $3d_{x^2-y^2}$ electron in each layer, $t_{x^2-y^2,z^2}$ is the intra-layer hybridization of

the $3d_{x^2-y^2}$ electron and $3d_{z^2}$ electrons between the nearest neighbors and the signs for the vertical and horizontal directions are opposite,[15] and $\mu_{x^2-y^2}$ and μ_{z^2} are the chemical potentials for the $3d_{x^2-y^2}$ and $3d_{z^2}$ orbitals of nickels, respectively. Here μ_{z^2} should be much smaller than $\mu_{x^2-y^2}$ to ensure that the $3d_{z^2}$ orbital is near half-filling, while the $3d_{x^2-y^2}$ orbital is close to quarter-filling. In this model, we have ignored the intra-layer (inter-layer) hopping for the $3d_{z^2}$ ($3d_{x^2-y^2}$) orbitals and double occupancy of the $3d_{z^2}$ orbital is not allowed, i.e., the local constraint $n^d_{a,i} = n^d_{a,i,\uparrow} + n^d_{a,i,\downarrow} < 2$ has been imposed. Actually this effective bi-layer model Hamiltonian is different from the single orbital bi-layer Hubbard model,[19–27] and the distinct low-energy physics can be expected.

When the intra-layer hybridization between two orbitals $t_{x^2-y^2,z^2}$ is absent, the $3d_{z^2}$ orbitals are decoupled with the $3d_{x^2-y^2}$ orbitals. Because the intra-layer hopping of the $3d_{z^2}$ orbitals can be neglected, the ground state of the two-site half-filled $3d_{z^2}$ orbitals is an isolated singlet. The filling of $3d_{x^2-y^2}$ is close to $n^c = 1/2$ per lattice site, so the ground state of the interacting $3d_{x^2-y^2}$ electrons behave as a paramagnetic metal. With a finite hybridization $t_{x^2-y^2,z^2}$, the $3d_{z^2}$ electrons can hop on the lattice, and the isolated pairs of the $3d_{z^2}$ electrons can gain coherence and the system may display superconductivity in the large inter-layer coupling limit. This picture shares a similarity to the superconductivity theory of the metallization of σ-bonding band.[17,18]

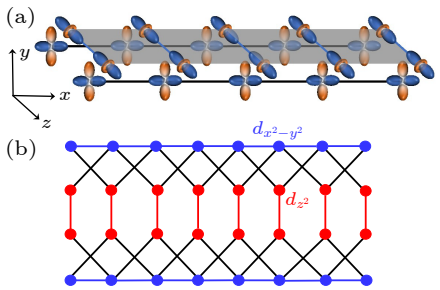

Fig. 2. (a) The minimum setup to capture the double-layer structure of $La_3Ni_2O_7$. (b) The lattice model used in the DMRG calculation. Red and blue dots represent the $3d_{z^2}$ and $3d_{x^2-y^2}$ orbitals, respectively. We set the inter-layer hopping of $3d_{z^2}$ orbital (t_{z^2}, red vertical lines) as the energy unit, and the hopping between $3d_{x^2-y^2}$ orbitals $t_{x^2-y^2} = 0.8$ (horizontal blue lines), the hybridization between the $3d_{z^2}$ and $3d_{x^2-y^2}$ orbitals $t_{x^2-y^2,z^2} = 0.4$ (black cross lines). The super exchange interaction between the inter-layer $3d_{z^2}$ orbitals is set as $J = 0.5$.

Numerical Results of DMRG Study. In order to explore the low energy physics of the effective model Eq. (4), we employ the DMRG method[28,29] to numerically solve a minimum one-dimensional setup which captures the double-layer structure with the length $L = 32$ as shown in Fig. 2. According to the DFT results,[15,16] we choose the hopping parameter t_{z^2} as the energy unit, and $t_{x^2-y^2} = 0.8$, $t_{x^2-y^2,z^2} = 0.4$. For the simplicity, we ignore the Hubbard repulsion for the $3d_{x^2-y^2}$ orbitals because they are far away from half-filling. Here we mainly focus on the large J limit, so the local antiferromagnetic spin coupling is set as $J = 0.5$. Under the averaged filling $n = 3/4$, we have a scan of $\Delta_\mu = \mu_{x^2-y^2} - \mu_{z^2}$ to ensure that the $3d_{z^2}$ orbitals are 1/16 hole doping away from half-filling and the $3d_{x^2-y^2}$ orbital electrons have 9/16 electron filling. With these chosen parameters, the $3d_{z^2}$ orbital electrons sit closely to the Mott-insulating limit, while the $3d_{x^2-y^2}$ orbital electrons are in the large doping limit, resembling the orbital selective Mott physics.[30] In our DMRG calculations, the maximal number of the states is kept up to $m = 18000$ with a truncation error $\epsilon < 5 \times 10^{-6}$. In the following, we will plot the numerical results with large kept states m to indicate the convergence of DMRG calculations.

In Fig. 3(a), we give the local charge density distributions in real space of both the $3d_{z^2}$ and $3d_{x^2-y^2}$ electrons along one row, and the numerical results for other rows have the same values. The obtained results with finite m display nice convergence. A CDW ordering with periodicity of 5 is clearly seen for the $3d_{z^2}$ orbital electrons, while there seems to be a CDW ordering with wavelength 3 for the $3d_{x^2-y^2}$ electrons, but the modulation is not as regular as that in the $3d_{z^2}$ orbitals.

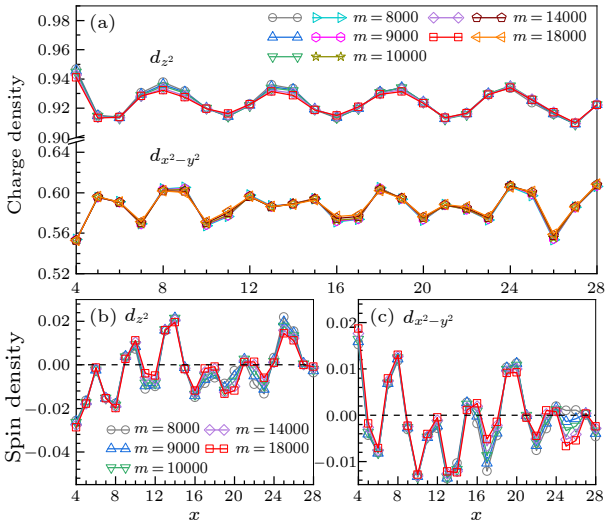

Fig. 3. (a) The charge density distribution of the $3d_{x^2-y^2}$ and $3d_{z^2}$ orbitals. The chemical potential difference Δ_μ is set 2.01 to target the 1/16 hole doping level on the $3d_{z^2}$ orbitals and 9/16 electron filling on the $3d_{x^2-y^2}$ orbital. The charge density wave pattern with wavelength 5 can be seen in the $3d_{z^2}$ orbitals, while the pattern of the charge oscillation in the $3d_{x^2-y^2}$ orbitals has a wavelength 3 roughly. [(b), (c)] The short-ranged spin density distribution of the $3d_{x^2-y^2}$ and $3d_{z^2}$ orbitals.

In the DMRG method, the calculation of the spin-spin correlations is more demanding. Thus we can also apply a pinning magnetic field with the strength $h_m = 0.5$ at one site in the left edge, which allows us to probe the magnetic structure by calculating the local spin density.[31] In Figs. 3(b) and 3(c), the local spin densities of both the $3d_{x^2-y^2}$ and $3d_{z^2}$ orbitals are displayed. Here the numerical results are shown for one row and the absolute values of the different rows are almost the same. We can see that the spin density of both orbital electrons is short-range (disordered), and the system exhibits a paramagnetic be-

havior.

In order to consider the superconductivity instability, we calculated the equal-time spin singlet superconducting pair–pair correlation function between bond i (formed by site $(i, 1)$ and $(i, 2)$) and bond j (formed by site $(j, 1)$ and $(j, 2)$), which is defined as $D(i, j) = \langle \hat{\Delta}_i^\dagger \hat{\Delta}_j \rangle$, where

$$\hat{\Delta}_i^\dagger = (\hat{c}^\dagger_{(i,1),\uparrow}\hat{c}^\dagger_{(i,2),\downarrow} - \hat{c}^\dagger_{(i,1),\downarrow}\hat{c}^\dagger_{(i,2),\uparrow})/\sqrt{2}. \quad (5)$$

We set the vertical $3d_{z^2}$ bond as the reference bond in the calculation of the pair–pair correlations. In Fig. 4(a), we show the numerical results for the $3d_{z^2}$ bonds, and find that the envelope of the pair–pair correlation displays an algebraically decay $|D(r)| \sim r^{-K_{\rm sc}}$ with exponent $K_{\rm sc} = 1.5(1)$. This pair–pair correlation is always positive and oscillated in real space, consistent with the strong local singlet pairings of the $3d_{z^2}$ electrons. On the other hand, for the $3d_{x^2-y^2}$ electrons, the envelope of this pair–pair correlation exhibits an algebraic decay with exponent $K_{\rm sc} = 0.74(7)$ displayed in Fig. 4(b). Moreover, this pair–pair correlation oscillates on the lattice with a special sign structure $+--$.

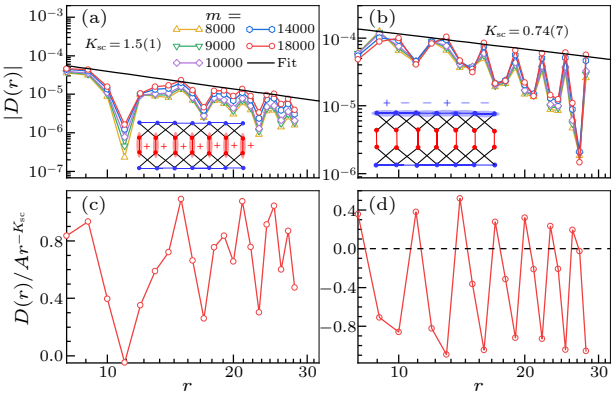

Fig. 4. The spin singlet pair–pair correlation functions for the minimum setup model. The inter-layer $3d_{z^2}$ bond at $x = 4$ is set as the reference bond in the calculation, and we can find oscillations with the same period with the charge density. (a) The pair–pair correlation decay for the inter-layer $3d_{z^2}$ bonds. The correlation is always positive, and the envelope fitting gives an algebraically decay with exponent $K_{\rm sc} = 1.5(1)$. (b) The pair–pair correlation decay for the $3d_{x^2-y^2}$ bonds has a periodic sign structure of $+--$. The envelope fitting gives an algebraically decay with exponent $K_{\rm sc} = 0.74(7)$. In (c) and (d), we display the pair–pair correlations divided by the fitted envelope functions in (a) and (b) to clearly show the sign and oscillation structure.

Since both the fitted exponents $K_{\rm sc}$ of the envelopes for $3d_{z^2}$ and $3d_{x^2-y^2}$ orbital electrons are smaller than 2, the SC correlations are strong enough so that a quasi-long-range order emerges, implying the divergence of the static pair–pair SC susceptibility characterized as

$$\chi_{\rm sc}(T) \sim T^{-(2-K_{\rm sc})}, \quad \text{when} \quad T \to 0. \quad (6)$$

Moreover, the pair–pair correlations for $3d_{x^2-y^2}$ orbital electrons exhibit oscillation with sign changes, so the emerged superconductivity may be regarded as a pair-density wave ordered state. We note that the intra-layer pairing for the $3d_{x^2-y^2}$ orbitals is stronger than the inter-layer pairing for the $3d_{z^2}$ orbitals. Though the inter-layer super-exchange favors the formation of singlets for the $3d_{z^2}$ orbital, these isolated singlets need to hybridize with the itinerant $3d_{x^2-y^2}$ orbital electrons to gain coherence. Therefore, it is reasonable that the intra-layer pairing is stronger than the inter-layer pairing, even though the latter is argued to be the origin of electron pairing in the system.

In summary, we have proposed an effective bi-layer model Hamiltonian to describe the low energy physics of high-$T_{\rm c}$ superconductivity $La_3Ni_2O_7$ under high pressure.[15] In this effective model, we have argued that the σ-bonding band formed from the $3d_{z^2}$ orbitals via the apical oxygen can be metalized due to the hybridization with the itinerant $3d_{x^2-y^2}$ orbitals, displaying unconventional high-$T_{\rm c}$ superconductivity. We have also performed DMRG study on a minimum one-dimensional setup with the length $L = 32$. The DMRG results show instability of CDW-modulated superconductivity. The dominant spin singlet pair–pair correlation is from the $3d_{x^2-y^2}$ orbitals, displaying a pair-density-wave quasi-long-range order. Though this numerical calculation for a minimum setup, we would like to argue that the obtained properties can be used to justify the validity of the proposed effective bi-layer model Hamiltonian for the understanding the high-$T_{\rm c}$ superconductivity in $La_3Ni_2O_7$ under high pressure.

Note Added. During the preparation of this work, several theoretical studies[32–37] appeared on arXiv and the electronic structures and possible pairing instabilities of the high-$T_{\rm c}$ superconductivity of $La_3Ni_2O_7$ under high pressure are independently discussed.

Acknowledgments. G. M. Zhang is grateful to Meng Wang and Fu-Chun Zhang for their useful discussions. Y. Shen and M. P. Qin thank Weidong Luo for his generosity to provide computational resources for this work. G. M. Zhang acknowledges the support from the National Key Research and Development Program of China (Grant No. 2017YFA0302902). M. P. Qin acknowledges the support from the National Key Research and Development Program of China (Grant No. 2022YFA1405400), the Innovation Program for Quantum Science and Technology (Grant No. 2021ZD0301902), the National Natural Science Foundation of China (Grant No. 12274290), and the Sponsorship from Yangyang Development Fund. All the DMRG calculations are carried out with iTensor library.[38]

References

[1] Li D F, Lee K, Wang B Y, Osada M, Crossley S, Lee H R, Cui Y, Hikita Y, and Hwang H Y 2019 *Nature* **572** 624
[2] Nomura Y and Arita R 2022 *Rep. Prog. Phys.* **85** 052501
[3] Li D F, Wang B Y, Lee K, Harvey S P, Osada M, Goodge B H, Kourkoutis L F, and Hwang H Y 2020 *Phys. Rev. Lett.* **125** 027001
[4] Zeng S W, Tang C S, Yin X M *et al.* 2020 *Phys. Rev. Lett.* **125** 147003
[5] Osada M, Wang B Y, Lee K, Li D, and Hwang H Y 2020 *Phys. Rev. Mater.* **4** 121801

[6] Osada M, Wang B Y, Goodge B H, Harvey S P, Lee K, Li D, Kourkoutis L F, and Hwang H Y 2021 *Adv. Mater.* **33** 2104083
[7] Zeng S W, Li C J, Chow L E, Cao Y, Zhang Z T, Tang C S, Yin X M, Lim Z S, Hu J X, Yang P *et al.* 2022 *Sci. Adv.* **8** eabl9927
[8] Anisimov V I, Bukhvalov D, and Rice T M 1999 *Phys. Rev. B* **59** 7901
[9] Lee K W and Pickett W E 2004 *Phys. Rev. B* **70** 165109
[10] Jiang M, Berciu M, and Sawatzky G A 2020 *Phys. Rev. Lett.* **124** 207004
[11] Ikeda A, Krockenberger Y, Irie H, Naito M, and Yamamoto H 2016 *Appl. Phys. Express* **9** 061101
[12] Zhang G M, Yang Y F, and Zhang F C 2020 *Phys. Rev. B* **101** 020501
[13] Wang Z, Zhang G M, Yang Y F, and Zhang F C 2020 *Phys. Rev. B* **102** 220501
[14] Wang N N, Yang M W, Yang Z, Chen K Y, Zhang H, Zhang Q H, Zhu Z H, Uwatoko Y, Gu L, Dong X L *et al.* 2022 *Nat. Commun.* **13** 4367
[15] Sun H, Huo M, Hu X, Li J, Liu Z, Han Y, Tang L, Mao Z, Yang P, Wang B, Cheng J, Yao D X, Zhang G M, and Wang M 2023 *Nature* **621** 493
[16] Pardo V and Pickett W E 2011 *Phys. Rev. B* **83** 245128
[17] Gao M, Lu Z Y, and Xiang T 2015 *Phys. Rev. B* **91** 045132
[18] Gao M, Lu Z Y, and Xiang T 2015 *Physics* **44** 421 (in Chinese)
[19] Dagotto E, Riera J, and Scalapino D 1992 *Phys. Rev. B* **45** 5744
[20] Bulut N, Scalapino D J, and Scalettar R T 1992 *Phys. Rev. B* **45** 5577
[21] Kuroki K, Kimura T, and Arita R 2002 *Phys. Rev. B* **66** 184508
[22] Maier T A and Scalapino D J 2011 *Phys. Rev. B* **84** 180513
[23] Mishra V, Scalapino D J, and Maier T A 2016 *Sci. Rep.* **6** 32078
[24] Nakata M, Ogura D, Usui H, and Kuroki K 2017 *Phys. Rev. B* **95** 214509
[25] Maier T A, Mishra V, Balduzzi G, and Scalapino D J 2019 *Phys. Rev. B* **99** 140504
[26] Karakuzu S, Johnston S, and Maier T A 2021 *Phys. Rev. B* **104** 245109
[27] Kato D and Kuroki K 2020 *Phys. Rev. Res.* **2** 023156
[28] White S R 1992 *Phys. Rev. Lett.* **69** 2863
[29] White S R 1993 *Phys. Rev. B* **48** 10345
[30] de'Medici L, Hassan S R, Capone M, and Dai X 2009 *Phys. Rev. Lett.* **102** 126401
[31] White S R and Chernyshev A L 2007 *Phys. Rev. Lett.* **99** 127004
[32] Luo Z H, Hu X W, Wang M, Wú W, and Yao D X 2023 *Phys. Rev. Lett.* **131** 126001
[33] Yang Q G, Wang D, and Wang Q H 2023 *Phys. Rev. B* **108** L140505
[34] Zhang Y, Lin L F, Moreo A, and Dagotto E 2023 arXiv:2306.03231 [cond-mat.supr-con]
[35] Lechermann F, Gondolf J, Botzel S, and Eremin I M 2023 arXiv:2306.05121 [cond-mat.str-el]
[36] Sakakibara H, Kitamine N, Ochi M, and Kuroki K 2023 arXiv:2306.06039 [cond-mat.supr-con]
[37] Gu Y, Le C, Yang Z, Wu X, and Hu J 2023 arXiv:2306.07275 [cond-mat.supr-con]
[38] Fishman M, White S R, and Stoudenmire E M 2022 *SciPost Physics Codebases 4*